

# Multi-way differential power divider with microstrip output interfaces

Cheng-Guang Sun<sup>1,2</sup>, Jia-Lin Li<sup>2</sup>, Baidenger Agyekum Twumasi<sup>2,3</sup>

The design and implementation of planar multi-way differential power dividers remain a challenge in terms of the compactness and especially, for the achievable characteristic impedance of the quarter-wavelength transformer when considering large number of outputs. In this work, the double-sided parallel stripline is recommended to realize such a power divider with out-of-phase outputs, and explicit design methods are provided. The proposed multi-way power divider was developed without the use of lump elements on a single substrate. For system applications, a prototype operating at 41.6 MHz with 12 pairs of out-of-phase outputs that utilize the microstrip line as the output interfaces was fabricated and examined. At the center frequency of 41.6MHz, the developed prototype measured insertion losses akin to 14.3 dB as compared with the theoretical data of 13.8 dB. The attainable impedance bandwidth ranges from 10 MHz to 80 MHz under a magnitude imbalance of  $\pm 0.3$  dB. The isolations of the adjacent outputs are about 13.1 dB as compared with the theoretical values of 14.428 dB, and are better than 34 dB for more distant ones. Parameter measurements are in good agreement with the numerical predications, thus demonstrating the realization of the proposed multi-way power divider.

**Key words:** power divider, multi-way, differential, microstrip

## 1 Introduction

As an important component of microwave circuit, power dividers has been extensively applied in electromagnetic signal transmission systems. The differential type of power divider allocates one input signal into multiple outputs, where each pair of outputs exhibits out-of-phase characteristics, and all outputs being equal in magnitude for most cases. Such a kind of structure find applications in power amplifiers, mixers and feeding networks of antenna arrays.

The design of multi-way power divider using different methods has been extensively studied by several researchers in recent years. Instead of conventional lumped resistors, a saw-tooth graphene flake is fabricated to obtain good isolation between arbitrary output ports [1]. A planar network with RLC and LC structures are introduced in a four-way power divider, and excellent impedance matching and output isolation can be realized [2]. In [3], the approach of balanced-to-single-ended and single-ended-to-balanced is adopted in 1-to- $2^n$  way power divider. Compared with balanced-to-balanced ones, the circuit size is effectively reduced. By using p-i-n diodes, an N-way reconfigurable power divider is constructed simply with low insertion loss and high isolation between transmission ports [4]. In [5], arbitrary power-dividing ratio for an N-way power divider is developed by using node voltage and current method. Based on microstrip-line Marchand balun, a multiple power divider is miniaturized, and out-of-phase outputs are achieved [6]. Lumped-elements

have been utilized in multi-way power divider to feature length-saving or filtering property [7, 8]. Capacitors can be added between the coupled lines to improve the return loss of outputs [9]. At low frequencies, the power divider is designed using lumped-elements to obtain size reduction or high isolation [10, 11]. However, the number of output ports are small, and the amplitude and phase differences between outputs fluctuates due to the tolerance of the lumped-elements.

This article presents a multi-way differential power divider with 12 pairs of differential outputs. The developed differential divider, based on the double-sided parallel stripline, uses the microstrip line as the outputs. This structure only uses a single substrate, thus facilitating the fabrication and assembling, and further, reducing the cost. In this work, the studied differential topology is first analyzed, and several explicit design equations are given as a guide for developing such a kind of multi-way power divider network. A prototype centered at 41.6 MHz, was fabricated and measured. Results indicate the examinations match well with the analysis, thus confirming the studied differential scheme and analysis method.

## 2 Topology and analyses

To obtain the out-of-phase outputs, the double-sided parallel stripline is adopted in this proposed multi-way power divider. As shown in Fig. 1, the same topology is

<sup>1</sup> Institute of Antenna and Microwave Techniques, Tianjin University of Technology and Education, Tianjin, China, <sup>2</sup> School of Physics, University of Electronic Science and Technology of China (UESTC), Chengdu, China, <sup>3</sup> Electrical and Electronic Engineering Department, Ho Technical University, Ho, Ghana, sunchengguang-23@sina.com, jialinli@uestc.edu.cn, btwumasi@htu.edu.gh

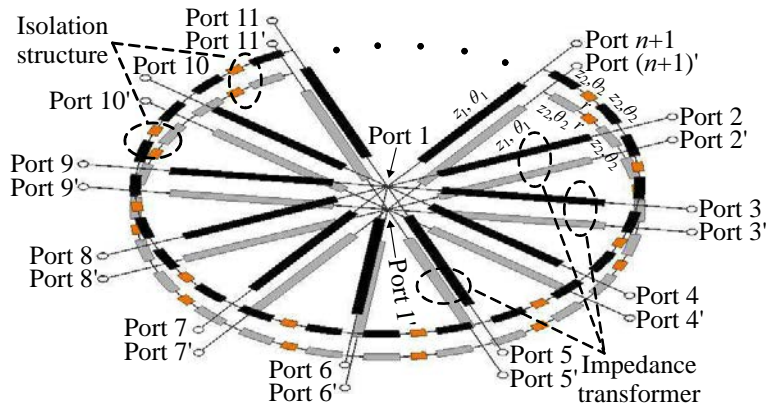


Fig. 1. Topology of the multi-way differential power divider, where the upper and lower structures are shown in black and gray

Assuming and denoting an identity matrix as  $E$ , the scattering matrix can be determined as [13, 14]

$$S = 2(E + \frac{1}{r}M^{-1} - (N + E)) \quad (2)$$

Where,  $M$  and  $N$  are  $n \times n$  matrix and given by

$$M = \begin{bmatrix} 2 & -1 & 0 & 0 & \dots & 0 & -1 \\ -1 & 2 & -1 & 0 & \dots & 0 & 0 \\ 0 & -1 & 2 & -1 & 0 & \dots & 0 \\ \vdots & 0 & \ddots & \ddots & \ddots & \ddots & \vdots \\ \vdots & \vdots & \ddots & \ddots & \ddots & \ddots & 0 \\ 0 & 0 & \dots & 0 & -1 & 2 & -1 \\ -1 & 0 & \dots & 0 & 0 & -1 & 2 \end{bmatrix} \quad (3)$$

$$N = \begin{bmatrix} \frac{1}{n} & \frac{1}{n} & \dots & \dots & \dots & \dots & \frac{1}{n} \\ \frac{1}{n} & \frac{1}{n} & \frac{1}{n} & \dots & \dots & \dots & \frac{1}{n} \\ \vdots & \ddots & \ddots & \ddots & \ddots & \ddots & \vdots \\ \vdots & \vdots & \ddots & \ddots & \ddots & \ddots & \vdots \\ \vdots & \vdots & \vdots & \ddots & \ddots & \ddots & \frac{1}{n} \\ \frac{1}{n} & \dots & \dots & \dots & \dots & \frac{1}{n} & \frac{1}{n} \end{bmatrix} \quad (4)$$

Fig. 2. Equivalent circuit of the studied power divider to analyze the isolation of a differential pair by omitting the closed-ring isolation structure

placed on the top and bottom side of a microwave substrate, including the impedance transformers and isolation structures. The inputs, named port 1 and port 1', are centrally located. The outputs – port 2 to port  $n + 1$  and port 2' to port  $(n + 1)'$  – are spread outwards in a star-shape distribution. The impedance transformer (normalized impedance and electrical length are marked as  $z_1$  and  $\theta_1$ ), composed of a pair of double-sided parallel stripline, is the key component used to attain the differential pairs. The isolation structure (marked as  $z_2$  and  $\theta_2$ ), with a lumped resistor  $r$  centered between two striplines, is connected with adjacent outputs. For such a kind of topology, when the impedance transformers are of quarter wavelengths at the center operation frequency, the normalized characteristic impedances for  $n$ -pair output ports are given by [12]

$$z_1 = \sqrt{2n} \quad (1)$$

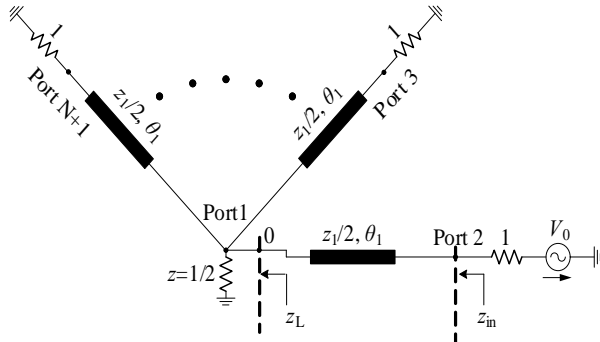
Figure 1 shows the layout of the proposed power divider network, showing impedance lines and the isolation structures as well as the input and multiple output ports for both upper and lower structures.

Notice that the above formulation is valid at the center operation frequency, and the transmission-line pair of the isolation structure (denoted by  $z_2$  and  $\theta_2$ ) as shown in Fig. 1 is omitted here as a result of its very small length compared to the quarter-wavelength transformer, i.e.,  $\theta_2 \ll \theta_1 = 90^\circ$ .

For the multiway-outputs (take 11- and 12-way for example), Tab. 1 shows scattering parameters under different conditions. It indicates that a matched output leads to relatively poor isolation between the adjacent ports, while ideal isolations between adjacent ports are achievable at the cost of very poor output return loss, which is less than 3 dB. By setting the output return loss equal to isolation between adjacent ports, a tradeoff can be approached.

**Table 1.** Scattering parameters of 11-way and 12-way outputs under different conditions, where  $i = 2, 3, \dots, 13$ 

| Number of pairs | Conditions            | Normalized r | Results: (Data in braces are in dB)   |
|-----------------|-----------------------|--------------|---|
| $n = 11$        | $S_{ii} = 0$          | 1.694        | $S_{i, i+1} = 0.23$ (12.767) $S_{i, i+2} = 0.004$ (49.171)<br>$S_{i, i+3} = 0.063$ (24.001) $S_{i, i+4} = 0.083$ (21.667)<br>$S_{i, i+5} = 0.088$ (21.13)<br>$S_{ii} = 0.718$ (2.882) $S_{i, i+2} = 0.086$ (21.276)                               |
|                 | $S_{i, i+1} = 0$      | 17.944       | $S_{i, i+3} = 0.091$ (20.85) $S_{i, i+4} = 0.091$ (20.829)<br>$S_{i, i+5} = 0.091$ (20.828)   |
|                 | $S_{ii} = S_{i, i+1}$ | 2.781        | $S_{ii} = S_{i, i+1} = 0.19$ (14.431) $S_{i, i+2} = 0.029$ (30.646)<br>$S_{i, i+3} = 0.077$ (22.224) $S_{i, i+4} = 0.088$ (21.118)<br>$S_{i, i+5} = 0.09$ (20.904)  |
| $n = 12$        | $S_{ii} = 0$          | 1.661        | $S_{i, i+1} = 0.239$ (12.441) $S_{i, i+2} = 0.012$ (38.114)<br>$S_{i, i+3} = 0.055$ (25.217) $S_{i, i+4} = 0.075$ (22.522)<br>$S_{i, i+5} = 0.081$ (21.874) $S_{i, i+6} = 0.082$ (21.741)<br>$S_{ii} = 0.742$ (2.592) $S_{i, i+2} = 0.08$ (21.99) |
|                 | $S_{i, i+1} = 0$      | 19.95        | $S_{i, i+3} = 0.08$ (21.602) $S_{i, i+4} = 0.08$ (21.584)<br>$S_{i, i+5} = 0.08$ (21.584) $S_{i, i+6} = 0.08$ (21.584)  |
|                 | $S_{ii} = S_{i, i+1}$ | 2.781        | $S_{ii} = S_{i, i+1} = 0.197$ (14.091) $S_{i, i+2} = 0.0218$ (33.239)<br>$S_{i, i+3} = 0.0698$ (23.118) $S_{i, i+4} = 0.0804$ (21.898)<br>$S_{i, i+5} = 0.0827$ (21.655) $S_{i, i+6} = 0.083$ (21.613)  |


**Fig. 3.** The odd-mode equivalent circuit to study the isolation of a differential pair

The isolation performances among differential pairs, *ie*  $S_{22'}$  in Fig. 1, are discussed here but, for simplicity, the closed-ring shaped isolation structure is not included in the analysis. When the output loads of all differential pairs are terminated as  $z_L = 1$ , its equivalent circuit can be described as shown in Fig. 2, showing the equivalent circuit of the studied power divider to analyze the isolation of a differential pair by omitting the closed-ring isolation structure.

In Fig. 2, the even- and odd-mode methods are used to analyze the isolation performance of the differential pair. For the even-mode excitation, in-phase sources are applied to ports 2 and 2', corresponding to inserting an infinite magnetic wall along the halved thickness of the substrate. In this case, the reflection coefficient of port 2 would be

$$\Gamma_{22e} = 1 \quad (5)$$

For the odd-mode excitation, anti-phase sources are applied to ports 2 and 2', corresponding to placing an electric wall along the halved thickness of the substrate. Thus, the stripline is reduced to the microstrip line with a halved thickness, where its odd-mode characteristic impedance  $z_{1o}$  would be [15]

$$z_{1o} = \frac{z_1}{2} \quad (6)$$

Figure 3 shows the odd-mode equivalent circuit to study the isolation of the differential pair.

In this case, the equivalent circuit shown in Fig. 2 can be further simplified as illustrated in Fig. 3, where the odd-mode reflection coefficient of port 2 is therefore given by

$$\Gamma_{22o} = \frac{z_{in} - 1}{z_{in} + 1} \quad (7)$$

where  $z_{in}$  is the input impedance at port 2 that is

$$z_{in} = \frac{z_1}{2} \frac{2z_L + jz_1 \tan \theta_1}{z_1 + j2z_L \tan \theta_1} \quad (8)$$

and  $z_L$  is the load impedance at the reference plane 0 and given by

$$z_L = \frac{1}{2} \parallel \frac{1}{N-1} \frac{z_1}{2} \frac{2 + jz_1 \tan \theta_1}{z_1 + j2 \tan \theta_1} \quad (9)$$

where symbol  $\parallel$  denotes the two components in parallel.

To this end, the isolation of a differential pair would be [12]

$$S_{22'} = \frac{\Gamma_{22e} - \Gamma_{22o}}{2} \quad (10)$$

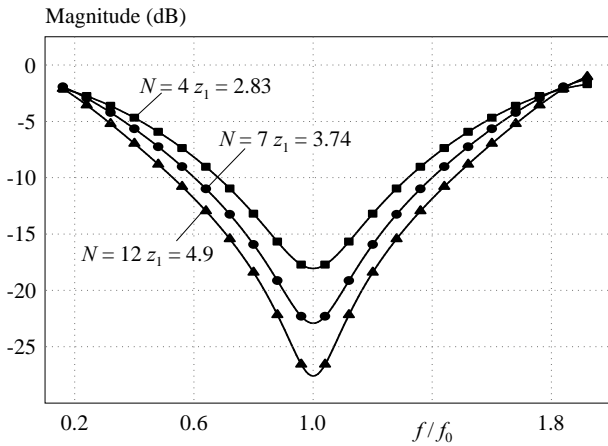


Fig. 4. The isolation of a differential pair for  $N = 4, 7,$  and  $12$  pairs

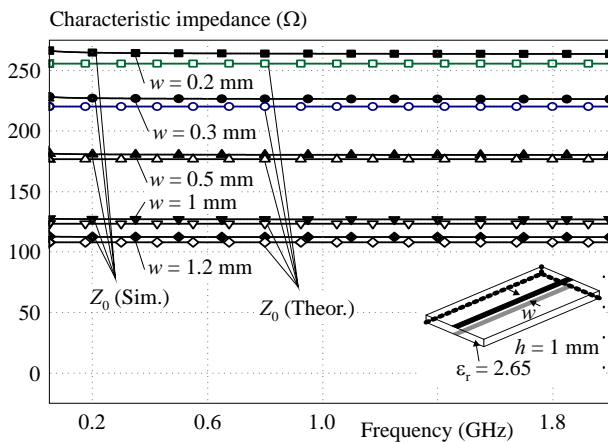


Fig. 5. Characteristic impedances of the broadside-coupled stripline under different line widths

Table 2. Physical parameters of the demonstrator (units: mm)

|              |             |              |             |           |
|--------------|-------------|--------------|-------------|-----------|
| $l = 83.6$   | $d = 24.9$  | $w_1 = 22.3$ | $w_2 = 0.3$ | $w_3 = 1$ |
| $w_4 = 0.75$ | $w_5 = 2.7$ | $w_6 = 1.2$  | $w_7 = 5.8$ | $w_8 = 1$ |

Here, we further specify 4-pair, 7-pair and 12-pair differential outputs to investigate the isolations of a differential pair. Figure 4 plots the calculated results based on the above discussions, where the normalized characteristic impedances,  $z_1$ , of the impedance transformer are respectively determined from (1). As shown in Fig. 4, good isolations are observed between a differential pair. Meanwhile, with the increase of the output pairs, the isolation can be further enhanced.

### 3 Design of power divider with 12 pair differential outputs

A prototype demonstrator is designed. The center operation frequencies is 41.6 MHz. Based on the above studies, the quarter-wavelength transformer has the characteristic impedance of  $Z_1 = \sqrt{24}Z_0 \approx 244.949 \Omega$ . Meanwhile, we choose  $S_{22} = S_{23}$  from Tab. 1 in this design,

thus the isolation resistors is  $R = 139.05 \Omega$  when referring to a system of  $Z_0 = 50 \Omega$  impedance.

Figure 5 shows the characteristic impedances of the broadside-coupled stripline under different line widths as indicated for both calculated and EM simulations.

Based on the studies by Wheeler [16], the characteristic impedances of the transformer pair for several line widths are calculated. Figure 5 records the calculated and electromagnetic (EM) simulated results, where full-wave EM simulator, Ansoft HFSS, is utilized and the microwave substrate has a relative permittivity of  $\epsilon_r = 2.65$  and a thickness of  $h = 1$  mm. It is observed from Fig. 5 that very high impedance ( $> 250 \Omega$ ) can be readily achieved by using this kind of transmission line, and the theoretical calculations presented by Wheeler is in good agreement with the EM simulations. Meanwhile, constant impedances were found within a wide frequency range, indicating its potential advantage for practical applications. From these results, the line width in this design is selected as  $w = 0.3$  mm by using the same substrate.

In Fig. 1, the transmission-line pair of the isolation structure denoted by  $z_2$  and  $\theta_2$  functions as bridging the isolation resistors among outputs. Hence, its length is designed to be as short as possible. It is achieved by meandering the radially distributed quarter-wavelength transformers, thus leading to compact designs. Notice that due to the complexity of analytic discussions on the closed-ring isolation network when involving the transmission-line pair, no analytic methods were constructed. Consequently, the design guide is initially set to  $z_2 = 2$  and  $\theta_2$  being small enough, while the exact determinations of  $z_2$  and  $\theta_2$  are based on the numerical calculations of the entire network. The small length,  $\theta_2$ , of the isolation network would introduce extra reactance to the impedance transformer, thus shifting the center operation frequency slightly, which can be shifted back by slightly tuning the length,  $\theta_1$ , of the transformer.

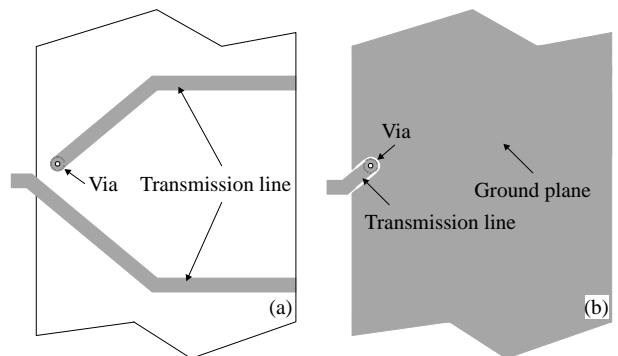
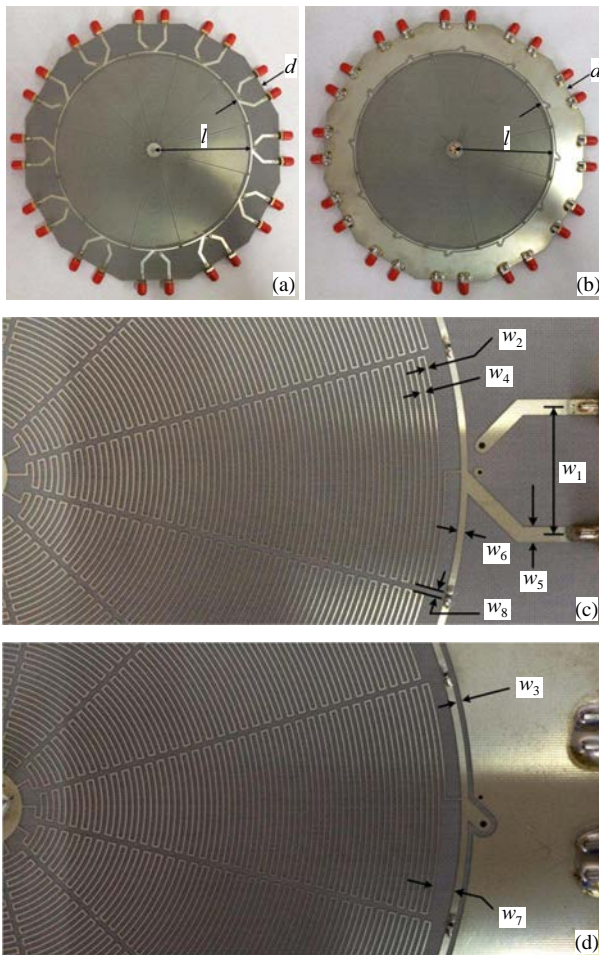


Fig. 6. Microstrip line based differential outputs. (a) – front side, (b) – back side

**Table 3.** Performance comparisons of power dividers

| Reference /Years | Central frequency (MHz) | Bandwidth (%) (return loss < 10 dB) | Number of ways | Number of layers | In phase or out-of-phase | Using lumped element |
|------------------|-------------------------|-------------------------------------|----------------|------------------|--------------------------|----------------------|
| (1)/2018         | 2400                    | 35.4                                | 9              | 2                | in phase                 | no                   |
| (2)/2018         | 1000                    | 50                                  | 4              | 1                | in phase                 | no                   |
| (3)/2016         | 1800                    | 36.1                                | 8              | 1                | out-of-phase             | no                   |
| (4)/2017         | 5000                    | 40                                  | 4              | 2                | in phase                 | no                   |
| (5)/2019         | 3450                    | 49.3                                | 6              | 2                | in phase                 | no                   |
| (6)/2019         | 3400                    | 85.3                                | 4              | 1                | out-of-phase             | no                   |
| (7)/2018         | 1000                    | 90                                  | 8              | 1                | in phase                 | yes                  |
| (9)/2018         | 1510                    | 34.4                                | 4              | 1                | in phase                 | yes                  |
| (10)/2013        | 435                     | 39                                  | 5              | 1                | in phase                 | yes                  |
| This work        | 41.6                    | 40                                  | 24             | 1                | out-of-phase             | no                   |



**Fig. 7.** Photographs of the developed demonstrator: (a) – front side. (b) – back side, (c) – Details of the front side, (d) – details of the back side

The differential outputs of this demonstrator are the microstrip lines. Fig. 6. Shows microstrip line based differential outputs. It is realized by transiting the transmission line of the back side to the front side with the use of vertical interconnections, as shown in Fig. 6.

#### 4 Numerical calculations and experimental results

Based on the above analyses, the required characteristic impedance of the transformer for 12-pair differential outputs is  $\sqrt{24}Z_0 \approx 244.949 \Omega$ . This corresponds to a line width of  $w = 0.3 \text{ mm}$  on the substrate mentioned above, as plotted in Fig. 5. The  $50 - \Omega$  microstrip transmission lines are set as line width of  $2.7 \text{ mm}$ . Figure 7 shows the photographs of the developed demonstrator, the front and the backside.

The radially distributed transformers are meandered for miniaturization, as illustrated in Fig. 7(c). The centrally placed input port is connected with a coaxial cable, where circular disks with optimal radials at both front and back sides of the substrate were optimized for impedance matching and for assembling (soldering). All impedance transformers start with the circular disks. The isolation resistors are all commercially available values of  $150 \Omega$ , as compared with the theoretical values of  $139.05 \Omega$ . Thus, the theoretical results based on (2) to (4) would be  $S_{ii} = 12.919 \text{ dB}$ ,  $S_{i, i+1} = 14.428 \text{ dB}$ ,  $S_{i, i+2} = 31.601 \text{ dB}$ , ( $i = 2, \dots, 13$ ). When referred to Tab. 1, it is seen that, the output return losses are slightly degraded under the condition of  $S_{22} = S_{23}$ . The full-wave EM simulator, Ansoft HFSS, was used to perform the numerical calculations. With optimal simulations, it was found that the transmission-line pair of the isolation network has a length of  $\theta_2 = 1.8^\circ$  and line impedance of  $Z_2 = 113.2 \Omega$ . It is seen  $\theta_2$  is small enough as compared with  $\theta_1$ , thus confirming the approximate discussions presented above. Table 2 lists physical parameters when referring to Fig. 7.

Photographs of the fabricated demonstrator are shown in Figs. 7(a)-(d), the front and back sides as well as the details of the both. The measurements were carried out by using Agilent N9918A network analyzer. The simulation and experiment results are shown in Fig. 8. From the return losses for the input and output ports described in

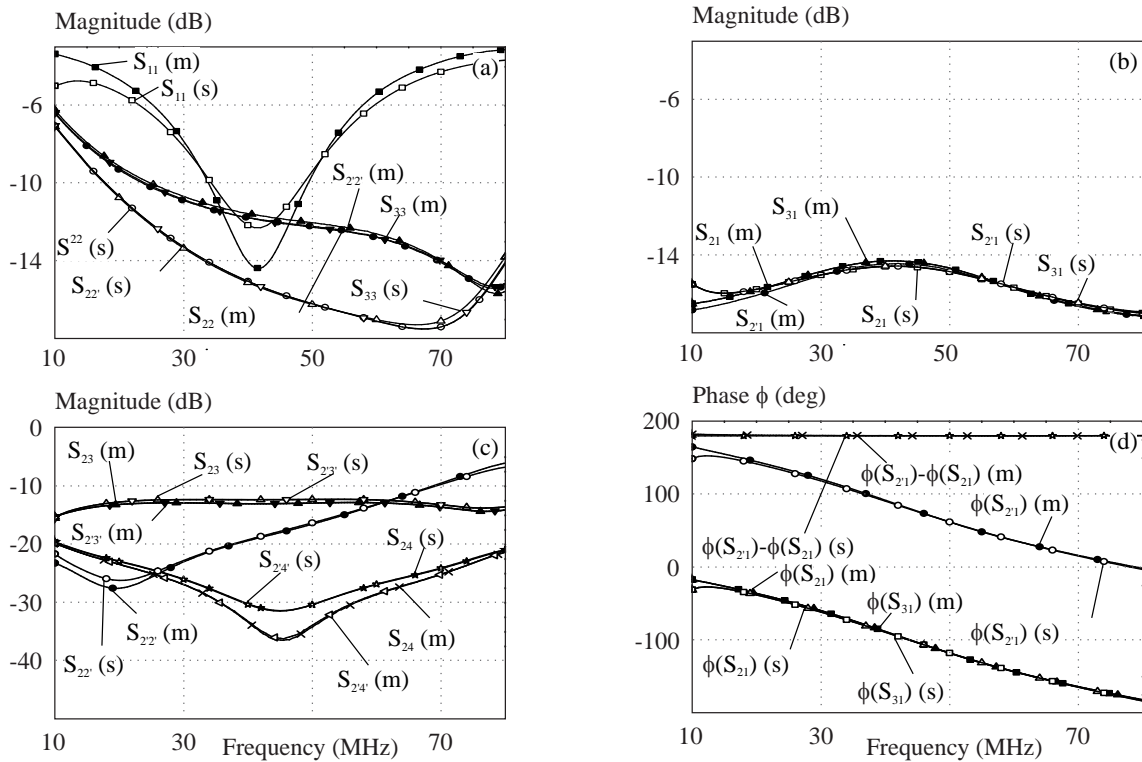


**Fig. 8.** Simulated (s) and measured (m) results of the demonstrator: (a) – return losses, (b) – insertion losses, (c) – port isolation, (d) – phase responses

Fig. 8(a), it can be seen that the power divider works at the center frequency of 41.6 MHz. Although the outputs are not well matched, the return losses are over 10 dB within a wide range to meet technical requirements for applications. At the center frequency shown in Fig. 8(b), measured insertion losses are approximately 14.3 dB compared with the theoretical data of 13.8 dB. The operation band is from 10 MHz to 80 MHz under a magnitude imbalance of  $\pm 0.3$  dB. As shown in Fig. 8(c), the isolations of the adjacent outputs, namely  $S_{23}$  or  $S_{23'}$ , are approximately 13.1 dB as compared with the theoretical values of 14.428 dB, while for  $S_{24}$  and  $S_{24'}$ , they are better than 34 dB. The isolations of the separated outputs could be further enhanced and not detailed here for brevity. From 10 MHz to approximately 60 MHz, the isolation of a differential pair,  $S_{22'}$ , is better than 13 dB with the best value being over 27 dB. Fig. 8(d) records the out-of-phase results. The range of  $180^\circ$  phase difference is from 10 MHz to 80 MHz in terms of an imbalance of  $\pm 2.5^\circ$ . Compared with the previous work [17], measured results indicate that this kind of power divider can also achieve a wide band by using microstrip output interfaces, thus showing the flexibility and compatibility with different system applications.

Table 3 lists some reported power dividers and the proposed contribution for performance comparisons. Compared with other works, this demonstrator exhibits a relatively more out-of-phase outputs and a broad operation

bandwidth. Meanwhile, the studied architecture is simple and easy to be integrated for system applications.

## 5 Conclusion

A multi-way differential power divider has been researched and a prototype developed in this paper. The out-of-phase power output was achieved using the double-sided parallel stripline and specific design approach has been provided. The output interfaces corresponding to the microstrip line were studied. A 12-pair differential output prototype with central frequency of 41.6 MHz was fabricated and measured. Experimental results are in good agreement with the numerical predictions (simulations). The developed differential power divider can be potentially applied to some industrial electronic systems for several applications.

### Acknowledgments

This work was supported by the Development Foundation of Tianjin University of Technology and Education (Grant KJ1919).

### REFERENCES

- [1] B. Wu, Y. Zhang, Y. Zhao, W. Zhang, and L. He, "Compact nine-way power divider with omnidirectional resistor based on graphene flake", *IEEE Microwave and Wireless Components Letters*, vol. 28, no. 9, pp. 762-764, September 2018.

- [2] T. Yu, J.-H. Tsai, and Y. Chang, "A radial four-way power divider with the proposed isolation network", *IEEE Microwave and Wireless Components Letters*, vol. 28, no. 3, pp. 194-196, Mar. 2018.
- [3] J. Shi, K. Xu, W. Zhang, J.-X. Chen, and G. Zhai, "An approach to 1-to- $2^n$  way microstrip balanced power divider", *IEEE Transaction on Microwave Theory and Techniques*, vol. 64, no. 12, pp. 4222-4231, December 2016.
- [4] H. Fan, X. Liang, J. Geng, L. Liu, and R. Jin, "An N-way reconfigurable power divider", *IEEE Transaction on Microwave Theory and Techniques*, vol. 65, no. 11, pp. 4122-4137, November 2017.
- [5] H. Chen, Y. Zhou, T. Zhang, W. Che, and Q. Xue, "N-way Gysel power divider with arbitrary power-dividing ratio", *IEEE Transaction on Microwave Theory and Techniques*, vol. 67, no. 2, pp. 659-669, February 2019.
- [6] K. Song, J. Yao, C. Zhong, and S. R. Patience, "Miniaturised wideband four-way out-of-phase power divider based on Marchand balun", *IET Microwaves, Antennas & Propagation*, vol. 13, Iss. 15, pp. 2682-2686, November 2019.
- [7] T. Yu, "Design of length-saving multiway Wilkinson power dividers", *IEEE Access*, vol. 6, pp. 14093-14105, Mar. 2018.
- [8] C. Zhu, J. Xu, W. Kang, and W. Wu, "Four-way microstrip lumped-element reconfigurable dual-mode filtering power divider", *IEEE Transactions on industrial electronics*, vol. 65, no. 3, Mar. 2018.
- [9] C. Zhu, J. Xu, and W. Wu, "Microstrip four-way reconfigurable single/dual/wideband filtering power divider with tunable frequency, bandwidth, and PDR", *IEEE Transactions on industrial electronics*, vol. 65, no. 11, November 2018.
- [10] A. Kosc, A. D. Maria, M. Limbach, R. Horn, and A. Reigber, "A 5 way lumped-elements Wilkinson power divider", *Proceeding of European Conference on Antenna and Propagation (EuCAP)*, Gothenburg, pp. 357-360, April 2013.
- [11] T. Zhang, W. Che, H. Chen, and W. Feng, "A Compact four-way dual-band power divider using lumped elements", *IEEE Microwave and Wireless Components Letters*, vol. 25, no. 2, pp. 94-96, February 2015.
- [12] D. M. Pozar, *Microwave Engineering*, 3rd Ed., New York, Wiley, 2009, chs.4, 8.
- [13] A. A. M. Saleh, "Planar electrically symmetric n-way hybrid power dividers/combiners", *IEEE Transaction on Microwave Theory and Techniques*, vol. MTT-28, no.6, pp. 555-563, June 1980.
- [14] A. A. M. Saleh, "Computation of the frequency response of a class of symmetric n-way power dividers", *The Bell System Technical Journal*, vol. 59, no.8, pp. 1493-1512, Oct. 1980.
- [15] S.-G. Kim and K. Chang, "Ultrawide-band transitions and new microwave components using double-sided parallel-strip lines", *IEEE Transaction on Microwave Theory and Techniques*, vol. 52, no. 9, pp. 2148-2152, Sept. 2004.
- [16] H. A. Wheeler, "Transmission-line properties of parallel strips separated by a dielectric sheet", *IEEE Transaction on Microwave Theory and Techniques*, vol. MTT-13, no.2, pp. 172-185, Mar. 1965.
- [17] C. G. Sun and J. L. Li, "Design of planar multi-way differential power division network using double-sided parallel stripline", *Electronics Letters*, vol. 53, no. 20, pp. 1364-1366, September 2017.

Received 9 May 2020

**Cheng-Guang Sun** was born at Tianjin, China, in 1980. He received the BS degree in Electronic Engineering in 2003 from the Hebei University of Technology, Tianjin, China, and MS degree in Physical Electronics in 2006 from the Hebei University of Technology, Tianjin, China, and PhD degree in Radio Physics in 2018 from the University of Electronic Science and Technology of China (UESTC), Chengdu, China. From April 2006 to August 2013, he was a teacher with the Institute of Antenna and Microwave Techniques, Tianjin University of Technology and Education, Tianjin, China. Since September 2018, he was an associate professor with the Institute of Antenna and Microwave Techniques, Tianjin University of Technology and Education, Tianjin, China. His research interests include microwave circuits and systems, time reversal electromagnetics.

**Jia-Lin Li** was born at Sichuan, China, in 1972. He received the MS degree from the University of Electronic Science and Technology of China (UESTC), Chengdu, China, in 2004, and the PhD degree from the City University of Hong Kong, Hong Kong, in 2009, both in electronic engineering. From September 2005 to August 2006, he was a Research Associate with the Wireless Communication Research Center, City University of Hong Kong, Hong Kong. Since September 2009, he has been with the School of Physical Electronics, UESTC, where he is currently a Professor. His research interests include the novel wireless electromagnetic communications, microwave/millimeter-wave antennas, circuits and systems, time reversal electromagnetics, and so on. He received the ICMMT Best Paper Award in 2012 International Conference on Microwave and Millimeter Wave Technology (ICMMT), the Outstanding Performance Award for Research Degree Students in the Academic Year 2007-2008 from the City University of Hong Kong, and the APMC Champion Prize at the 2008 Asia-Pacific Microwave Conference.

**Baidenger Agyekum Twumasi** was born at Nsawam, Ghana in 1981. He received the HND in Electrical/Electronic Engineering from Ho Technical University (Ho Polytechnic) in 2001, the ME degree in Telecom Management from the HAN University of Applied Sciences, Netherlands in 2011 and the PhD in Engineering (Electronic Science and Technology) from the University of Electronic Science and Technology of China in 2020. He is now with the University of Electronic Science and Technology of China (UESTC) as a post-doctoral researcher in the school of Physics. He has been with the Electrical/Electronic Engineering department of Ho Technical University (HTU), Ho in Ghana since February, 2008. His current research interests include antennas and propagation, Electromagnetic time reversal applications, circuits and systems.